HHS Public Access

Author manuscript

Mol Oncol. Author manuscript; available in PMC 2017 February 01.

Published in final edited form as:

Mol Oncol. 2016 February ; 10(2): 272–281. doi:10.1016/j.molonc.2015.10.007.

Endothelial Robo4 suppresses breast cancer growth and metastasis through regulation of tumor angiogenesis

Helong Zhao[1], **Dinesh K. Ahirwar**[1], **Steve Oghumu**[1], **Tasha Wilkie**[1], **Catherine A. Powell**[1], **Abhay R. Satoskar**[1], **Dean Y. Li**[2], and **Ramesh K. Ganju**[1,*]

[1]Department of Pathology, The Ohio State University Wexner Medical Center

[2]School of Medicine and Eccles Institute of Human Genetics, The University of Utah

Abstract

Targeting tumor angiogenesis is a promising alternative strategy for improvement of breast cancer therapy. Robo4 (roundabout homolog 4) signaling has been shown to protect endothelial integrity during sepsis shock and arthritis, and inhibit Vascular Endothelial Growth Factor (VEGF) signaling during pathological angiogenesis of retinopathy, which indicates that Robo4 might be a potential target for angiogenesis in breast cancer. In this study, we used immune competent Robo4 knockout mouse model to show that endothelial Robo4 is important for suppressing breast cancer growth and metastasis. And this effect does not involve the function of Robo4 on hematopoietic stem cells. Robo4 inhibits breast cancer growth and metastasis by regulating tumor angiogenesis, endothelial leakage and tight junction protein zona occuldens protein - 1 (ZO-1) downregulation. Treatment with SecinH3, a small molecule drug which deactivates ARF6 downstream of Robo4, can enhance Robo4 signaling and thus inhibit breast cancer growth and metastasis. SecinH3 mediated its effect by reducing tumor angiogenesis rather than directly affecting cancer cell proliferation. In conclusion, endothelial Robo4 signaling is important for suppressing breast cancer growth and metastasis, and it can be targeted (enhanced) by administrating a small molecular drug.

Keywords

Robo4; breast cancer; angiogenesis; ZO-1; tight junction

[*]Corresponding author: Ramesh K. Ganju, Ph.D., 810 BRT, 460 W 12th Ave, Columbus OH 43210, Ph: 614-292-5539, Fax: 614-247-0051, Ramesh.Ganju@osumc.edu.

Conflict of interest:

DYL is the co-founder of Navigen, Inc. and Recursion Pharmaceuticals, LLC. The other authors disclose no potential conflicts of interest.

Introduction

In current breast cancer treatment, frequent somatic mutation and heterogeneity of cancer cells have often rendered aggressive tumors resistant to chemotherapy (Gascoigne and Taylor, 2008; Gerlinger et al., 2012). Given the important supportive function and the rarity of mutation of tumor blood vessel endothelium, inhibiting tumor angiogenesis by targeting tumor endothelial cells has been considered an alternative strategy to overcome drug resistance. Tumor angiogenesis is necessary for tumor growth and it also promotes metastasis (Horak et al., 1992; Weidner et al., 1991). Angiogenesis can be initiated by chemoattractive and proliferative cytokines in the tumor environment, such as Vascular Endothelial Growth Factor (VEGF), which induces endothelial cell migration and proliferation (Ferrara, 2002). In addition, tumor derived inflammatory cytokines, such as IL-1β and CCL2, causes leakage of endothelium by disrupting the tight junction molecules, such as ZO-1, and in turn promotes endothelial sprouting during angiogenesis (Bolton et al., 1998; Salcedo et al., 2000; Stamatovic et al., 2003; Voronov et al., 2003). Moreover, defective endothelial integrity promotes breast cancer metastasis, especially when tight junction protein ZO-1 is degraded in tumor endothelial cells (Martin and Jiang, 2009; Zhou et al., 2014).

Robo4 is one of the cell surface receptors for the secreted signaling protein, Slit2 (Park et al., 2003). Its expression is restricted to endothelial cells and their progenitor, hematopoietic stem cells (HSCs) (Huminiecki et al., 2002; Smith-Berdan et al., 2011). Slit2-Robo4 signaling counteracts VEGF signaling and IL-1β signaling in endothelial cells to inhibit angiogenesis during retinopathy and protect endothelial integrity during sepsis shock (Jones et al., 2008; London et al., 2010). It has also been shown that Robo4 regulates HSC homing to bone marrow during HSC transplant (Smith-Berdan et al., 2011), and is important for vascularization during mammary gland development (Marlow et al., 2010). However, a recent report showed that the genetic depletion of Robo4 in endothelial cells does not affect the Slit2 binding and proposed Robo1 and Robo2 as preferred receptors for Slit2 activity (Rama et al., 2015). Although, the interaction of Slit2 and Robo4 in pathological angiogenesis has been a controversy, the role of Robo4 in breast cancer angiogenesis is not very well understood.

Recently, it was shown that the main signaling event of Robo4 pathway is the deactivation of a GTPase, ARF6 (Jones et al., 2009). Deactivation of ARF6 could be achieved by pharmacologically inhibiting ARF6 activating proteins, guanine nucleotide exchange factors, with the small molecule drug SecinH3 (Grossmann et al., 2013; Zhu et al., 2012). This drug has been shown to be effective in enhancing Robo4 function in treating arthritis and endotoxemia (Davis et al., 2014; Zhu et al., 2012). Hence, we hypothesize that SecinH3 also enhances Robo4 signaling in regulating breast cancer angiogenesis.

In the present study, we elucidated the role of endothelial Robo4 in breast cancer growth and metastasis by knocking out endothelial Robo4 and by enhancing Robo4 downstream signaling, and explored the possibility of using a novel small molecule drug to target Robo4 in the development of treatment against breast cancer.

Methods and Materials

Cells

PyMT cells were cultured in DMEM:F12 medium supplemented with 10% FBS and 1% dual antibiotics. E0771 and their subclones, E0.1 and E0.2, were cultured in complete RPMI 1640 or DMEM medium as indicated. Human microvascular endothelial cells (HMVEC) were cultured in ECM medium (ScienCell, San Diego, CA). MDA-MB-231 was cultured in DMEM medium. Cancer cell supernatant was collected from sub-confluent cultures after 48 h of serum starvation.

Animal study

Robo4$^{+/-}$ C57BL/6 mice (generated by Dr. Dean Li, University of Utah) were bred for Robo4$^{+/+}$ and Robo4$^{-/-}$ genotyped female mice. At 8-week age, 2×10^6 PyMT cells, or 0.2×10^6 E0771, E0.1, E0.2 cells in 50% Matrigel (Corning, MA) were injected into the right mammary fat pad of mice of all groups. For all animal studies, 5 to 8 mice were used in each group. For drug treatment experiments, mice were injected daily i.p. with 1mg/kg SecinH3 in PBS with 5% DMSO, or vehicle control, from the 2nd day after tumor injection. Tumor size was assessed once a week using a caliper and tumor volume was calculated according to the formula: volume = length × (width)^2/2. Mice were sacrificed at the end of study as shown in the figures or per the request of the veterinarian. All mice were kept in OSU's animal facility in compliance with the guidelines and protocols approved by the IACUC.

Cell proliferation assay

Cell proliferation assay was performed using Cell Proliferation Kit I (MTT) from Roche (Indianapolis, IN) per the kit manual. Proliferation assays were done in triplicates. 5×10^3 cells were plated in each well of a 96-well plate, and drug treatment was added to the cell at the time of plating. Cells were allowed to grow for 3 days, and cell numbers were quantified on each day. For quantifying cell number, MTT was added to the cells at day of measuring, and cells were lyzed with SDS solution after 12 hours. O.D. values were measured using Model 680 microplate reader from BIO-RAD (Hercules, CA).

Immunohistochemistry (IHC) and immunofluorescence staining

Tumor samples were fixed with 4% paraformaldehyde, processed and embedded in paraffin. Standard immunohistochemical techniques were used according to the manufacturer's recommendations (Vector Laboratories) using antibodies against CD31 (Santa Cruz 1:100), Vectastain Elite ABC reagents (Vector Laboratories), avidin DH:biotinylated horseradish peroxidase H complex with 3,3′-diaminobenzidine (Polysciences) and Mayer's hematoxylin (Fisher Scientific). For immunofluorescence staining, CD31 and Occludin primary antibodies and Alexa 488/568 secondary antibodies (Life Technologies, NY) were used for labelling.

Flow cytometry

Briefly, tumors isolated from the mice were chopped into fine pieces and digested into single cell suspensions at 37°C using Collagenase IV PBS solution (Life Technologies).

After passing through 0.45μm filters, cells were fixed in 4% paraformaldehyde in PBS. Surface proteins were stained with specific Alexa Fluor 488/568–conjugated Abs (Biolegend). Intracellular proteins were stained with specific primary Abs coupled with Alexa Fluor 488/568–conjugated secondary Abs (Life Technologies) after permeablization with Fixation/Permeabilization Solution Kit (BD Biosciences). Data were acquired using a FACSCalibur (BD Biosciences) and analyzed using CellQuest 5.0 software.

Western Blotting (WB)

WB was performed as previously discribed (Zhao et al., 2014). Briefly, proteins in cell lysates were separated by electrophoresis using NuPAGE SDS-PAGE Gel (Life Technologies). Proteins were transferred onto nitrocellulose membranes and blotted by specific primary and HRP-conjugated secondary Abs. Protein expression was detected by Thermo ECL reagents using X-ray films.

Quantitative-Reverse-Transcription-PCR (qRT-PCR)

qRT-PCR was performed as previously discribed (Zhao et al., 2014). Total RNA was extracted from cells using TRIzol reagent (Life Technologies) and purified with an RNeasy kit (QIAGEN). Total RNA was then reverse transcribed into cDNA using a High Capacity cDNA Reverse Transcription Kit (Life Technologies). Real-time PCR was then performed on an Eppendorf Mastercycler realplex using Power SYBR Green Master Mix (Life Technologies). Data analysis was performed using the standard "ΔΔCt method."

Statistical analysis

Reported data for cell line studies are the means ± S.E.M. of three independent biological samples. Animal studies use n= 5–8 mice for each group. The statistical significance was determined by the Student's t test or as specified. All the *in-vitro* experiments were repeated three times (N=3) and representative data have been presented.

Results

Endothelial Robo4 suppresses tumor growth and metastasis

In female C57BL/6 mice, orthotopic tumors of E0.2 (E0771 cell subclone generated in our lab) breast cancer cells developed significantly faster in Robo4$^{-/-}$ mice, compared to Robo4$^{+/+}$ mice (Figure 1A, B). The numbers of lung metastasis were also significantly greater in Robo4$^{-/-}$ mice (Figure 1C). Importantly, the probability of distal metastasis is known to be positively correlated with the primary tumor size (Koscielny et al., 1984). Thus, to eliminate the factor of tumor size from the influences on the number of lung metastatic foci, we analyzed the tumors on the Metastasis-Log$_{10}$Volume plot, in which the slope of linear regression indicates the aggressiveness of the breast tumors (Koscielny et al., 1984). On the Metastasis-Log$_{10}$Volume plot, the tumors in Robo4$^{-/-}$ mice are more aggressive in generating distal lung metastasis (Figure 1D). This is reflected by the significantly prolonged relapse free survival (RFS) of breast cancer patients with high Robo4 expression in a large combined cohort (Figure 1E). Taken together, we showed that Robo4 expression on endothelial cells inhibits breast cancer growth and metastasis.

Endothelial Robo4 suppresses tumor angiogenesis and protects vascular integrity

Robo4 is expressed only on endothelial cells and HSCs. Both endothelial cells and HSC-derived leukocytes can affect tumor development. By comparing the peripheral blood leukocyte profiles between wildtype ($Robo4^{+/+}$) and Robo4 knockout ($Robo4^{-/-}$) mice, we showed that Robo4 knockout did not affect the HSCs differentiation or the relative composition of peripheral blood leukocytes (Figure 2A–B). In addition, Robo4 was not expressed on breast cancer cells (Figure 2C). Thus, we hypothesized that Robo4 deficiency in endothelial cells, rather than HSCs, affects breast cancer development.

Vascular staining showed that there was more angiogenesis in the tumors of $Robo4^{-/-}$ mice, compared to $Robo4^{+/+}$ mice (Figure 3A). The increased vascular staining was coupled by a similar increase in the percentage of $CD31^{+}CD45^{-}$ tumor endothelial cells (Figure 3B). Disrupted tumor endothelial integrity not only initiates neovascularization, but also directly promotes cancer cell vascular invasion and metastasis. In endothelial Robo4-deficient mice, there is significantly increased percentage of branching phenotype, in addition to the increased tumor blood vessel quantity (Figure 4A). As a characteristic of angiogenesis and disrupted integrity, the increased branching in $Robo4^{-/-}$ tumor blood vessels was accompanied by the reduced level of tight junction associated protein, ZO-1, in tumor endothelial cells (Figure 4B). Accordingly, tight junction protein Occludin, which is stabilized by ZO-1, was also downregulated in tumor endothelial cells with Robo4 knockout (Figure 4C). These data showed that endothelial Robo4 suppresses tumor growth and metastasis by protecting endothelial integrity and angiogenesis.

Pharmacological enhancement of Robo4 signaling downstream of Robo4 inhibits tumor angiogenesis, tumor growth and metastasis

The small molecule drug, SecinH3, can enhance Robo4 signaling through deactivating the ARF6 activating proteins downstream of Robo4. SecinH3 treatment did not inhibit the *in vitro* proliferation of a non-aggressive murine breast cancer cell line, PyMT (Figure 5A). However, SecinH3 significantly reduced tumor growth of PyMT-cell orthotopic tumors *in vivo* (Figure 5B–C), without affecting the body condition of the mice (Figure 5D). This showed that SecinH3, with low toxicity, reduced tumor growth by influencing the host, rather than tumor cells. To further analyze the effect of Robo4 enhancement by SecinH3 on breast cancer metastasis, we used the highly aggressive murine breast cancer cell line, E0.1 (an E0771 subclone derived in our lab, Figure 6A–C). Again, SecinH3 significantly suppressed tumor growth of E0.1 cells (Figure 6D). More importantly, SecinH3 significantly inhibited lung metastasis of E0.1 tumors (Figure 6E). Judging by its Metastasis-Log_{10}Volume plot, SecinH3 reduced the aggressiveness (slope of linear regression) of E0.1 tumors (Figure 6F). Moreover, SecinH3 treatment rescued breast cancer cell supernatant induced loss of ZO-1 protein and mRNA in endothelial cells (Figure 7A–B). And accordingly, in both PyMT tumors and E0.1 tumors, SecinH3 treatment suppressed tumor angiogenesis and the branching phenotype (Figure 7C–D). Taken together, these data showed that, in accordance with the functions of Robo4, enhancing Robo4 signaling using small molecule drug (SecinH3) can inhibit breast tumor growth and metastasis by reducing tumor angiogenesis.

Discussion

Targeting tumor angiogenesis in breast cancer is considered an alternative treatment that may avoid problems of cancer cell heterogeneity and has long been investigated. Robo4 signaling has been shown to protect endothelial integrity during sepsis shock and prevent pathological angiogenesis in retinopathy (Jones et al., 2008; London et al., 2010). Robo4 has also been shown to inhibit VEGF signaling during mammary gland development (Marlow et al., 2010). Thus, targeting Robo4 signaling seems promising in inhibiting tumor angiogenesis in breast cancer. Previous reports have implied the importance of Robo4 in regulating angiogenesis (Jones et al., 2008; Koch et al., 2011; Park et al., 2003). In the present study, we used immune competent Robo4 knockout mouse model to show that Robo4 is important for suppressing breast cancer growth and metastasis (summarized in Figure 8). Moreover, knocking out Robo4 in HSCs did not affect the HSC differentiation or the leukocyte profile of the mice. Thus, endothelial Robo4 should be responsible for the anti-cancer effects observed in our study.

Robo4 knockout led to enhanced tumor angiogenesis. This is in agreement with previous works showing that Robo4 counteracts VEGF signaling in endothelial cells (Jones et al., 2008; Koch et al., 2011; Marlow et al., 2010). Importantly, more blood vessels showed the branching phenotype in Robo4$^{-/-}$ tumors. The sprouting induced branching of tumor blood vessels is caused by decrease of tight junctions and increase of endothelium leakage (Carmeliet and Jain, 2011). And reduced tight junction protein ZO-1 expression and increased leakage of endothelium have been shown to promote tumor angiogenesis and metastasis (Zhou et al., 2014). Indeed, we also observed a decrease of ZO-1 and its associated Occludin protein in Robo4$^{-/-}$ tumor endothelium, which should at least partly contribute to the enhanced angiogenesis and metastasis.

In this study, we used two subclones of C57BL/6 derived breast cancer cell line E0771, E0.1 and E0.2. They were generated in our lab by culturing isolated E0771 tumor cells in RPMI 1640 and DMEM media, respectively. E0.1 has less cell-to-plastic attachment, and generates bigger tumors and more lung metastasis in mice than E0.2 cells (Figure 6B, C). It has been suggested that lower environmental pH, increased glucose metabolism and less cell attachment favor cancerous progression of tumor cells. Comparing to DMEM, RPMI 1640 has less pH buffering capacity, less glucose and less calcium. Thus, it is possible that RPMI 1640 is more likely to promote cancerous progression (evolution) of tumor cells than DMEM. We chose to use E0.2 to study tumor growth and E0.1 to study lung metastasis for *in vivo* experiments. The reasons for increased aggressiveness of breast cancer cells in RPMI 1640 may be due to its less pH buffering capacity and lower glucose and calcium concentrations.

To confirm the role of Robo4, we investigated the effect of enhancing Robo4 signaling with the small molecule drug (SecinH3) which targets downstream of Robo4. Similar to previous studies of sepsis and arthritis (Davis et al., 2014; Zhu et al., 2012), SecinH3 showed robust effects on enhancing Robo4 signaling. It rescued tight junction protein ZO-1 expression and inhibited breast tumor angiogenesis, tumor growth and metastasis. Interestingly, SecinH3 did not inhibit the *in vitro* proliferation of PyMT and E0.1 breast cancer cells, except for

excessively high concentration. And Robo4 was not expressed in any of the breast cancer cell lines we used (Figure 2C). In addition, by using the analysis (Metastasis-Log_{10}Volume plot) of cancer aggressiveness in lung metastasis study, we eliminated the factors of cell proliferation and tumor size in determining influences of metastatic potential. These findings confirmed that SecinH3 acts on the host not the cancer cells *in vivo*.

When considering the therapeutic application of targeting Robo4 signaling, although increased tight junction between endothelial cells can counteract with breast cancer angiogenesis and metastasis, it may also affect other vascular systems away from the cancerous lesions. Anti-VEGF therapy has been shown to pose threat to maintenance of normal microvasculature (Kamba and McDonald, 2007). So it is not impossible that globally increased tight junctions also affect normal endothelial functions. In addition, some also argue that increased tight junctions in the blood brain barrier may also affect the essential supplies to the brain.

In conclusion, endothelial Robo4 is important for controlling tumor angiogenesis and endothelial leakage, which suppresses the growth and metastasis of breast cancer. The small molecule drug, SecinH3, can inhibit breast cancer growth and metastasis by enhancing Robo4 signaling. Although targeting Robo4 has been shown to be promising in treatment of sepsis shock (London et al., 2010), to date, the quest for Robo4 targeting strategy has been limited to injection of large doses of recombinant Slit2 (~120 kDa) protein (London et al., 2010), which is far from a good drug candidate. Hence, targeting ARF6 downstream of Robo4 with small molecular drug SecinH3 seems a promising alternative strategy.

Supplementary Material

Refer to Web version on PubMed Central for supplementary material.

Acknowledgments

The authors would like to thank Dr. Tsowin Hai (Ohio State University) for sharing the PyMT cell line; thank Mohd W. Nasser for technical support; thank Grace Amponsah and Angel B. Algarin for experimental assistance. This work is supported in part by the NIH grants R01 CA109527, CA153490 and R21 AI091420 to RKG, and Pelotonia Fellowship to HZ.

Abbreviations

VEGF	Vascular Endothelial Growth Factor
ZO-1	Zonula Occludens Protein-1 (Tight Junction Protein 1, TJP1)
ARF6	ADP-Ribosylation Factor 6
HSC	Hematopoietic Stem Cell
HMVEC	Human Microvascular Endothelial Cell
IHC	Immunohistochemistry
qRT-PCR	quantitative-Reverse-Transcription-PCR
WB	Western Blotting

RFS Relapse Free Survival

References

Bolton SJ, Anthony DC, Perry VH. Loss of the tight junction proteins occludin and zonula occludens-1 from cerebral vascular endothelium during neutrophil-induced blood-brain barrier breakdown in vivo. Neuroscience. 1998; 86:1245–1257. [PubMed: 9697130]

Carmeliet P, Jain RK. Molecular mechanisms and clinical applications of angiogenesis. Nature. 2011; 473:298–307. [PubMed: 21593862]

Davis CT, Zhu W, Gibson CC, Bowman-Kirigin JA, Sorensen L, Ling J, Sun H, Navankasattusas S, Li DY. ARF6 inhibition stabilizes the vasculature and enhances survival during endotoxic shock. J Immunol. 2014; 192:6045–6052. [PubMed: 24835390]

Ferrara N. VEGF and the quest for tumour angiogenesis factors. Nat Rev Cancer. 2002; 2:795–803. [PubMed: 12360282]

Gascoigne KE, Taylor SS. Cancer cells display profound intra- and interline variation following prolonged exposure to antimitotic drugs. Cancer Cell. 2008; 14:111–122. [PubMed: 18656424]

Gerlinger M, Rowan AJ, Horswell S, Larkin J, Endesfelder D, Gronroos E, Martinez P, Matthews N, Stewart A, Tarpey P, et al. Intratumor heterogeneity and branched evolution revealed by multiregion sequencing. N Engl J Med. 2012; 366:883–892. [PubMed: 22397650]

Grossmann AH, Yoo JH, Clancy J, Sorensen LK, Sedgwick A, Tong Z, Ostanin K, Rogers A, Grossmann KF, Tripp SR, et al. The small GTPase ARF6 stimulates β-catenin transcriptional activity during WNT5A-mediated melanoma invasion and metastasis. Sci Signal. 2013; 6:ra14. [PubMed: 23462101]

Győrffy B, Lanczky A, Eklund AC, Denkert C, Budczies J, Li Q, Szallasi Z. An online survival analysis tool to rapidly assess the effect of 22,277 genes on breast cancer prognosis using microarray data of 1,809 patients. Breast Cancer Res Treat. 2010; 123:725–731. [PubMed: 20020197]

Horak ER, Leek R, Klenk N, LeJeune S, Smith K, Stuart N, Greenall M, Stepniewska K, Harris AL. Angiogenesis, assessed by platelet/endothelial cell adhesion molecule antibodies, as indicator of node metastases and survival in breast cancer. Lancet. 1992; 340:1120–1124. [PubMed: 1279332]

Huminiecki L, Gorn M, Suchting S, Poulsom R, Bicknell R. Magic roundabout is a new member of the roundabout receptor family that is endothelial specific and expressed at sites of active angiogenesis. Genomics. 2002; 79:547–552. [PubMed: 11944987]

Jones CA, London NR, Chen H, Park KW, Sauvaget D, Stockton RA, Wythe JD, Suh W, Larrieu-Lahargue F, Mukouyama YS, et al. Robo4 stabilizes the vascular network by inhibiting pathologic angiogenesis and endothelial hyperpermeability. Nat Med. 2008; 14:448–453. [PubMed: 18345009]

Jones CA, Nishiya N, London NR, Zhu W, Sorensen LK, Chan AC, Lim CJ, Chen H, Zhang Q, Schultz PG, et al. Slit2-Robo4 signalling promotes vascular stability by blocking Arf6 activity. Nat Cell Biol. 2009; 11:1325–1331. [PubMed: 19855388]

Kamba T, McDonald DM. Mechanisms of adverse effects of anti-VEGF therapy for cancer. Br J Cancer. 2007; 96:1788–1795. [PubMed: 17519900]

Koch AW, Mathivet T, Larrivée B, Tong RK, Kowalski J, Pibouin-Fragner L, Bouvrée K, Stawicki S, Nicholes K, Rathore N, et al. Robo4 maintains vessel integrity and inhibits angiogenesis by interacting with UNC5B. Dev Cell. 2011; 20:33–46. [PubMed: 21238923]

Koscielny S, Tubiana M, Lê MG, Valleron AJ, Mouriesse H, Contesso G, Sarrazin D. Breast cancer: relationship between the size of the primary tumour and the probability of metastatic dissemination. Br J Cancer. 1984; 49:709–715. [PubMed: 6733019]

London NR, Zhu W, Bozza FA, Smith MC, Greif DM, Sorensen LK, Chen L, Kaminoh Y, Chan AC, Passi SF, et al. Targeting Robo4-dependent Slit signaling to survive the cytokine storm in sepsis and influenza. Sci Transl Med. 2010; 2:23ra19.

Marlow R, Binnewies M, Sorensen LK, Monica SD, Strickland P, Forsberg EC, Li DY, Hinck L. Vascular Robo4 restricts proangiogenic VEGF signaling in breast. Proc Natl Acad Sci U S A. 2010; 107:10520–10525. [PubMed: 20498081]

Martin TA, Jiang WG. Loss of tight junction barrier function and its role in cancer metastasis. Biochim Biophys Acta. 2009; 1788:872–891. [PubMed: 19059202]

Park KW, Morrison CM, Sorensen LK, Jones CA, Rao Y, Chien CB, Wu JY, Urness LD, Li DY. Robo4 is a vascular-specific receptor that inhibits endothelial migration. Dev Biol. 2003; 261:251–267. [PubMed: 12941633]

Rama N, Dubrac A, Mathivet T, Ní Chárthaigh RA, Genet G, Cristofaro B, Pibouin-Fragner L, Ma L, Eichmann A, Chédotal A. Slit2 signaling through Robo1 and Robo2 is required for retinal neovascularization. Nat Med. 2015; 21:483–491. [PubMed: 25894826]

Salcedo R, Ponce ML, Young HA, Wasserman K, Ward JM, Kleinman HK, Oppenheim JJ, Murphy WJ. Human endothelial cells express CCR2 and respond to MCP-1: direct role of MCP-1 in angiogenesis and tumor progression. Blood. 2000; 96:34–40. [PubMed: 10891427]

Smith-Berdan S, Nguyen A, Hassanein D, Zimmer M, Ugarte F, Ciriza J, Li D, García-Ojeda ME, Hinck L, Forsberg EC. Robo4 cooperates with CXCR4 to specify hematopoietic stem cell localization to bone marrow niches. Cell Stem Cell. 2011; 8:72–83. [PubMed: 21211783]

Stamatovic SM, Keep RF, Kunkel SL, Andjelkovic AV. Potential role of MCP-1 in endothelial cell tight junction ‘opening’: signaling via Rho and Rho kinase. J Cell Sci. 2003; 116:4615–4628. [PubMed: 14576355]

Voronov E, Shouval DS, Krelin Y, Cagnano E, Benharroch D, Iwakura Y, Dinarello CA, Apte RN. IL-1 is required for tumor invasiveness and angiogenesis. Proc Natl Acad Sci U S A. 2003; 100:2645–2650. [PubMed: 12598651]

Weidner N, Semple JP, Welch WR, Folkman J. Tumor angiogenesis and metastasis--correlation in invasive breast carcinoma. N Engl J Med. 1991; 324:1–8. [PubMed: 1701519]

Zhao H, Anand AR, Ganju RK. Slit2-Robo4 pathway modulates lipopolysaccharide-induced endothelial inflammation and its expression is dysregulated during endotoxemia. J Immunol. 2014; 192:385–393. [PubMed: 24272999]

Zhou W, Fong MY, Min Y, Somlo G, Liu L, Palomares MR, Yu Y, Chow A, O’Connor ST, Chin AR, et al. Cancer-secreted miR-105 destroys vascular endothelial barriers to promote metastasis. Cancer Cell. 2014; 25:501–515. [PubMed: 24735924]

Zhu W, London NR, Gibson CC, Davis CT, Tong Z, Sorensen LK, Shi DS, Guo J, Smith MC, Grossmann AH, et al. Interleukin receptor activates a MYD88-ARNO-ARF6 cascade to disrupt vascular stability. Nature. 2012; 492:252–255. [PubMed: 23143332]

Highlights

- Endothelial Robo4 regulates breast cancer growth and metastasis.
- Robo4 modulates angiogenesis by controlling endothelial tight junctions.
- Targeting signaling downstream of Robo4 is a potential anti-angiogenic strategy.

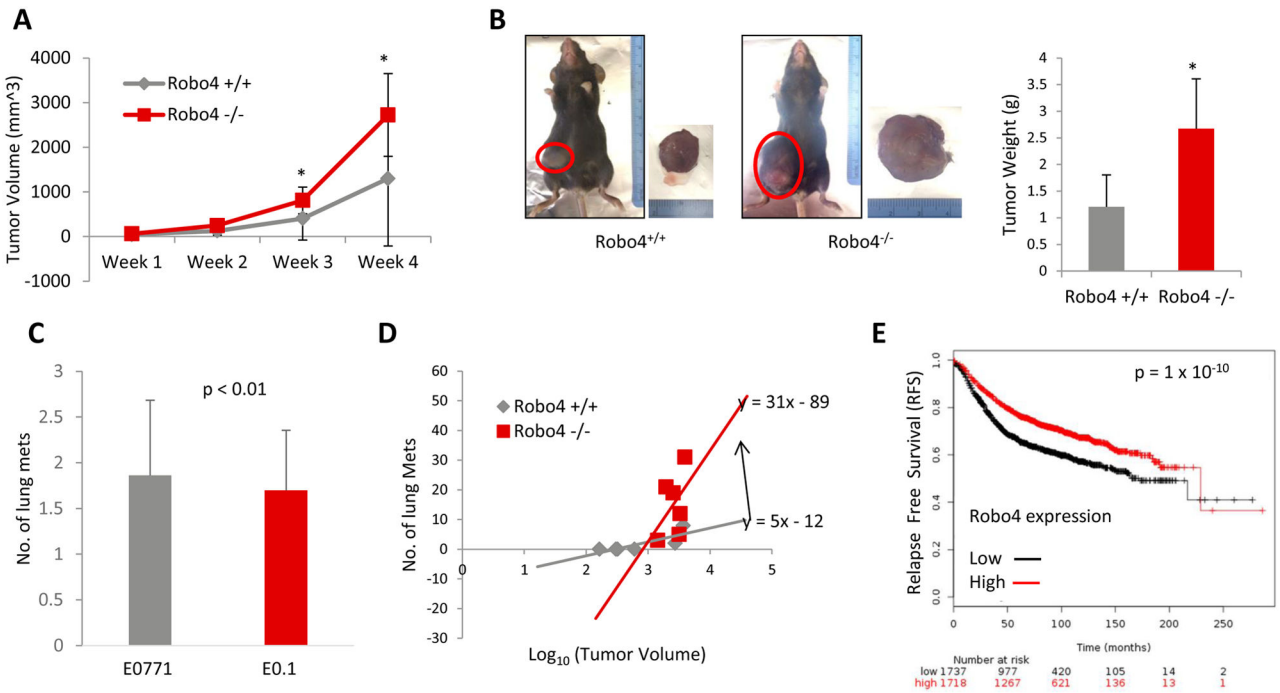

Figure 1. Endothelial Robo4 knockout enhanced breast cancer growth and metastasis

(A) Progression of tumor volumes of E0.2 tumors. **(B) Left:** Representative tumors of Robo4$^{+/+}$ and Robo4$^{-/-}$ mice at the end of the experiment, before sacrificing. **Right:** Tumor weight of Robo4$^{+/+}$ and Robo4$^{-/-}$ groups. **(C)** Number of lung metastasis in two groups (N=6 mice). **(D)** Metastasis-Log$_{10}$Volume plot of tumor and metastasis in two groups. Formula of linear regressions (in the form of: y = ax + b) were labelled by the lines. Slope is the value of a. N = 6 mice in each group. **(E)** Kaplan-Meier plot of RFS probability of breast cancers in a combined cohort of 3458 patients (Győrffy et al., 2010). Patients were separated by mean of Robo4 level. The two patient cohorts are compared by a Kaplan-Meier survival plot, and the hazard ratio with 95% confidence intervals and logrank P value are calculated. (*p<0.05)

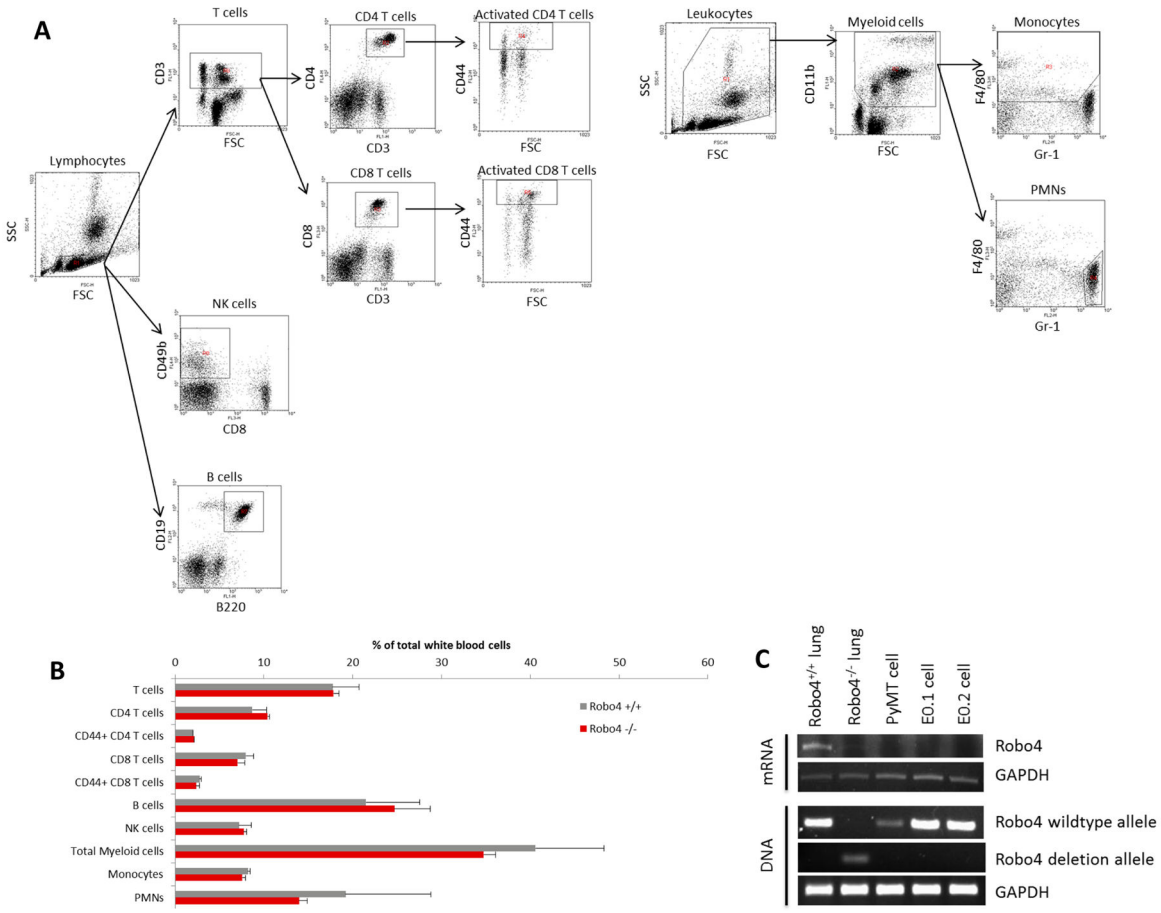

Figure 2. Host Robo4 knockout did not affect leukocyte differentiation and Robo4 is not expressed on tumor cells

(A) Gating strategy for analyzing peripheral blood leukocyte profiles by flow cytometry. Dot plots of flow cytometry analysis are shown, with the determined leukocyte population labelled on top. Polygonal areas in dot plots are the gates of selection. T cells: $CD3^+$; CD4 T cells: $CD3^+CD4^+$; CD8 T cells: $CD3^+CD8^+$; activated CD4/8 T cells: $CD3^+CD4/8^+CD44^{high}$; NK cells: $CD49b^+CD8^-$; B cells: $B220^+CD19^+$; Myeloid cells: $CD11b^+$; Monocytes: $CD11b^+F4/80^+Gr\text{-}1^-$; PMNs: $CD11b^+F4/80^-Gr^-1^+$. **(B)** Peripheral blood leukocyte profiling analysis. Peripheral blood of adult female $Robo4^{+/+}$ and $Robo4^{-/-}$ mice was collected into heparin solution, and red blood cells were lysed. White blood cells were then stained with conjugated antibodies against cell surface markers (Biolegend, CA) and analyzed by flow cytometry. There was not any significant difference between the peripheral blood leukocyte profiles of $Robo4^{+/+}$ and $Robo4^{-/-}$ mice. N = 6 mice were analyzed in each group. **(C)** Total DNA and RNA were extracted using TRIzol per the manufacturor's instructions. Robo4 mRNA expression levels of breast cancer cells were analyzed by reverse transcription and PCR. Lung tissues from $Robo4^{+/+}$ and $Robo4^{-/-}$ mice are used as positive and negative controls. Genotyping was performed using the extracted DNA.

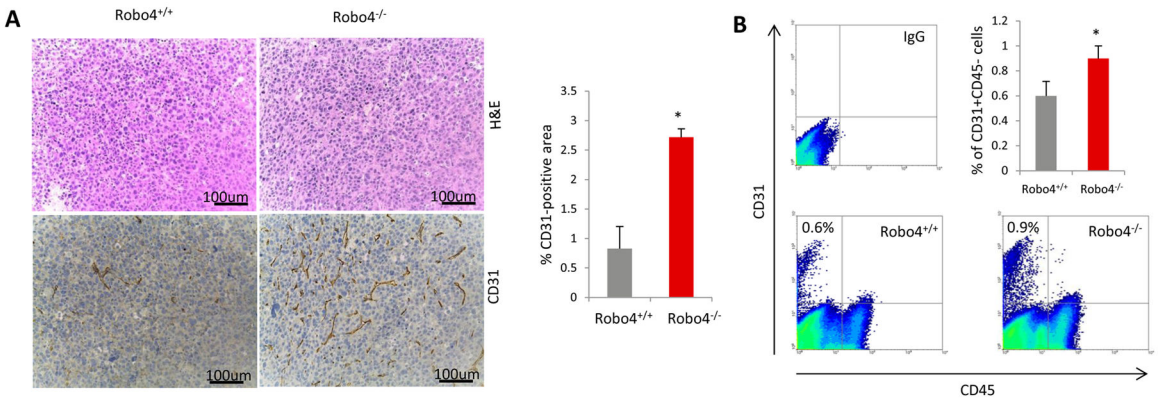

Figure 3. Endothelial Robo4 knockout led to increased tumor angiogenesis

(A) Left: H&E staining and IHC staining of tumor blood vessels (CD31) in E0.2 tumors of WT and Robo4$^{-/-}$ mice. **Right:** Quantitative analysis of the CD31 staining areas (n = 3). **(B)** Flow cytometry analysis of relative numbers of tumor endothelial cells. Tumors from each group were digested into single-cell suspensions using collagenase IV. Tumor endothelial cells (CD31^{+}CD45^{-}) were analyzed by flow cytometry. Statistical summary of 3 tumor samples from each group is shown in the bar graph of upper right panel.

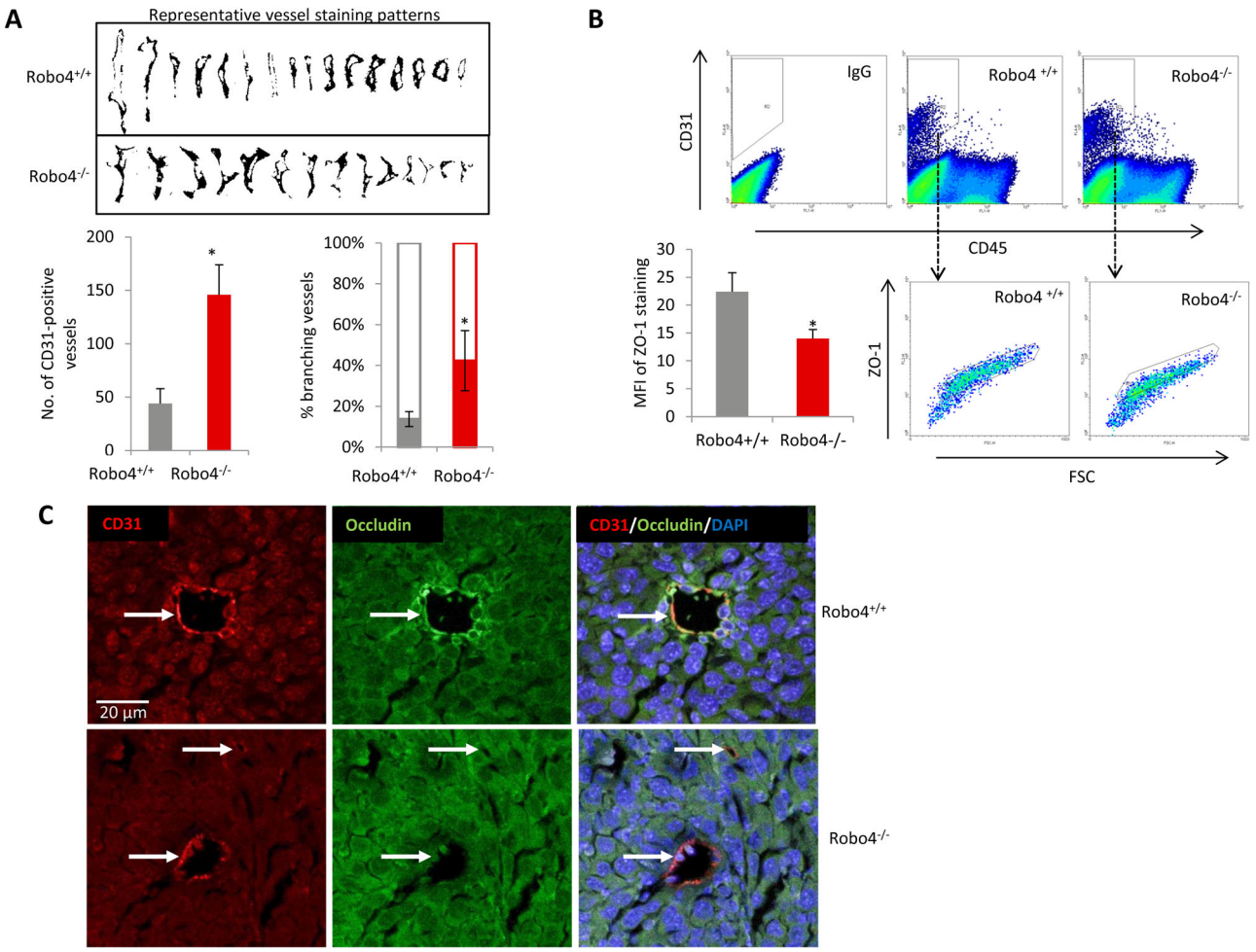

Figure 4. Increased angiogenesis in endothelial Robo4 knockout tumors is accompanied by perturbed endothelial integrity

(A) Upper: Representative vessel staining patterns of tumors in both groups. Patterns were isolated through adjusting color threshold of CD31 IHC images. **Lower-left:** Statistical summary of numbers of tumor blood vessels per field on IHC slides at 100x magnification. **Lower-right:** Percentage of branching tumor vessels of both groups. Branching is defined as the staining pattern with obvious lateral protrusions. **(B)** Flow cytometry analysis of tumor endothelial cell ZO-1 levels. Mean fluorescent intensity (MFI) is statistically summarized in the bar graph of lower left panel. **(C)** Representative immunofluorescence staining of tight junction protein, Occludin, on tumor blood vessels. CD31 is used as the endothelial cell marker, and DAPI is used as the nuclear marker. White arrows indicate blood vessels in the tumors. All images are to the same scale. (*$p<0.05$)

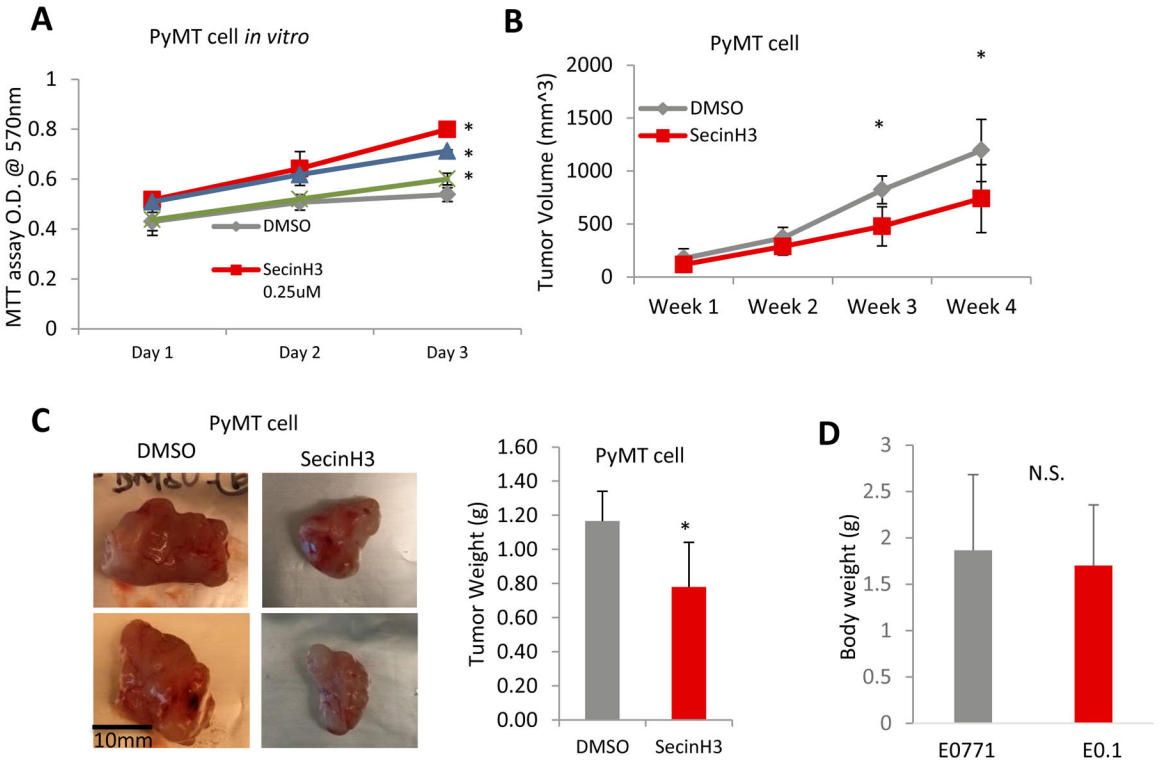

Figure 5. SecinH3 inhibited tumor growth, but not tumor cell proliferation

(A) MTT cell proliferation assays of SecinH3 treatment in PyMT cells in 96-well plates. SecinH3 relative dosage of *in vivo* experiments is about 2.2μM. **(B)** Tumor volume of PyMT tumor in C57BL/6 mice with or without SecinH3 treatment. N = 5 mice were analyzed in each group. **(C) Left:** Representative PyMT tumors of vehicle and SecinH3 treatment groups. **Right:** PyMT tumor weight at end of study. **(D)** Body weight of mice bearing PyMT tumors, with or without treatment of SecinH3. N = 5 mice were analyzed in each group. (*$p<0.05$, N.S.: non-significant)

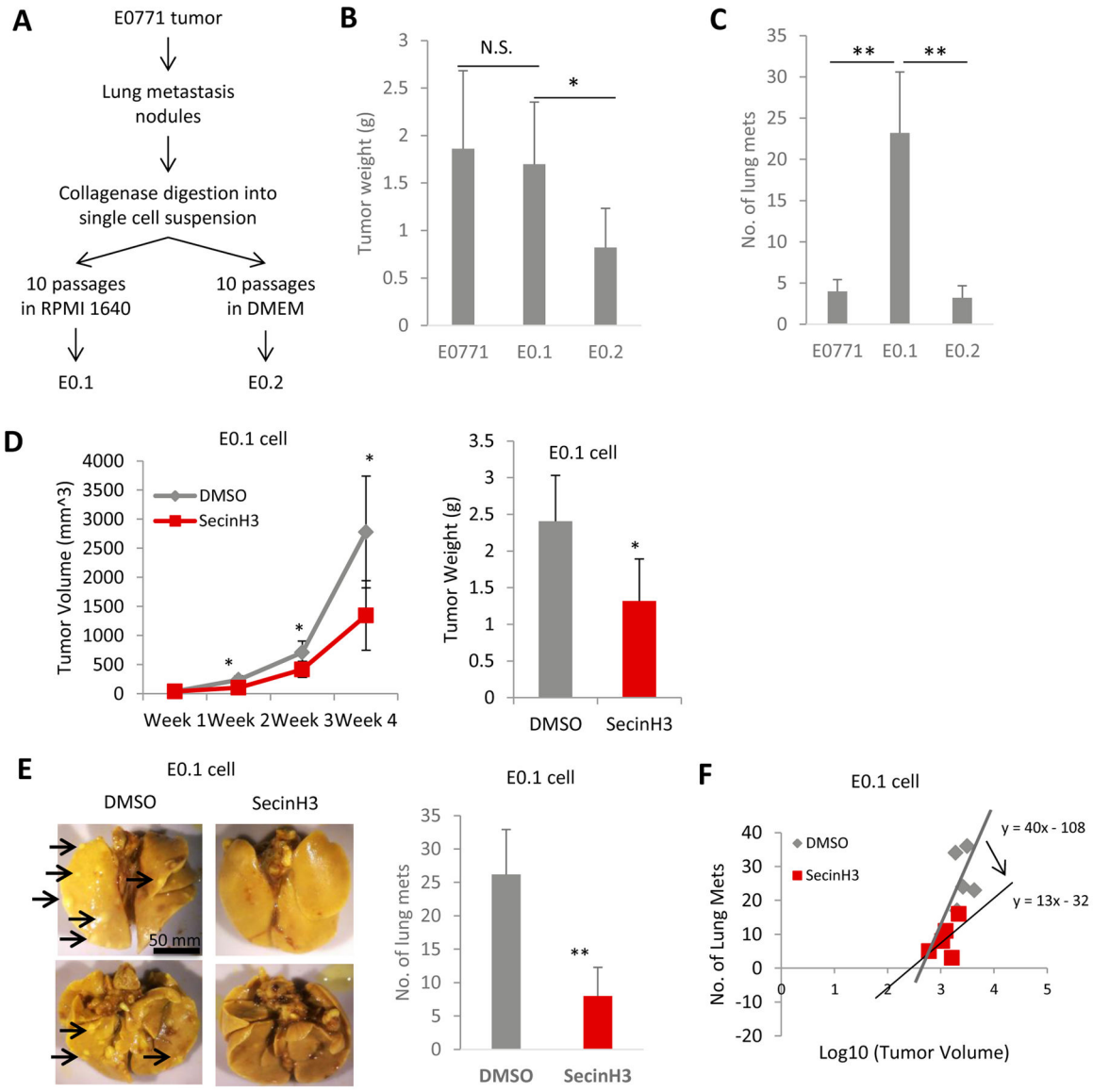

Figure 6. SecinH3 inhibited breast cancer lung metastasis

(A) Generation of E0.1 and E0.2 cell lines is described in the flow chart. After 10 passages of in vitro culture, E0.1 and E0.2 showed significantly different phenotypes. E0.1 proliferated faster, but had less attachment to the plate, comparing to E0.2. **(B and C)** When injecting same amount of E0771, E0.1 and E0.2 (0.2×10^6) cells into mouse mammary fat pads, E0.2 grew slower and E0.1 generated more lung metastasis than the other two (3 weeks post-injection). N = 5 mice each group. So E0.1 cell is considered highly aggressive, and E0.2 cell is considered less aggressive. **(D) Left:** Tumor volumes of E0.1 tumors in C57BL/6 mice with or without SecinH3 treatment. **Right:** E0.1 tumor weight at end of study. N = 5 mice were analyzed in each group. **(E) Left:** Representative lungs of mice bearing E0.1 tumors. Lungs were fixed with Bouin's solution so that metastatic foci appeared as white nodules (such as the ones pointed by arrows). All images are to the same scale. **Right:** Numbers of lung metastatic nodules of both groups. **(F)** Metastasis-

Log_{10}Volume plot of tumor and metastasis in two groups. (*p<0.05, **p<0.01, N.S.: non-significant)

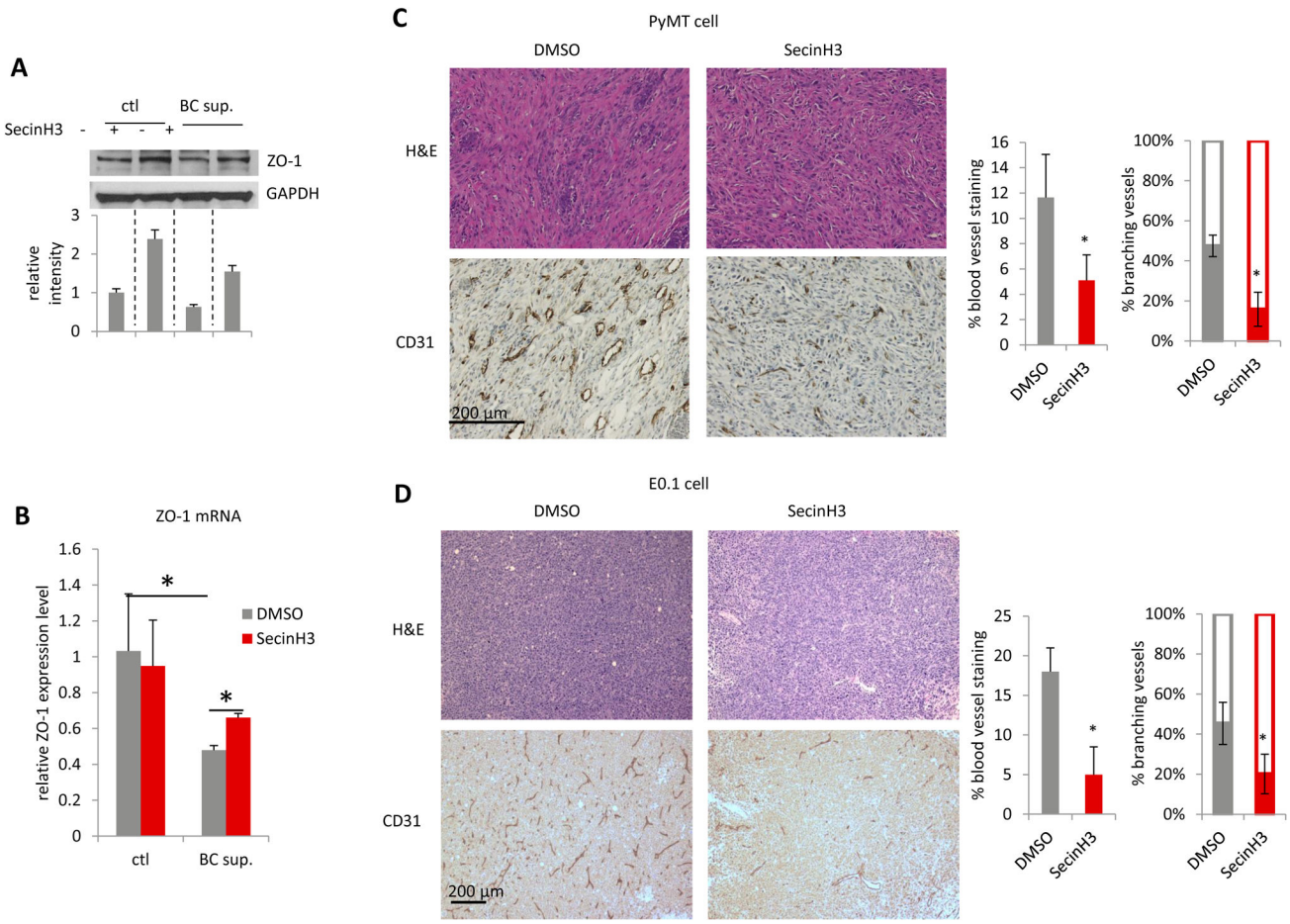

Figure 7. SecinH3 inhibited angiogenesis in PyMT and E0.1 tumors

(A and B) HMVEC cells were treated with supernatant of breast cancer cell MDA-MB-231 (BC sup.), with or without pre-treatment of 30μM SecinH3. ZO-1 protein **(A)** and mRNA **(B)** levels were analyzed by WB and qRT-PCR respectively. **(C and D) Left:** H&E and CD31 IHC staining of PyMT and E0.1 tumors. **Middle:** Quantification of CD31 staining area on slides of PyMT and E0.1 tumors. **Right:** Percentage of branching phenotype in tumor blood vessel staining. N = 3 mice were analyzed in each group. (*p<0.05)

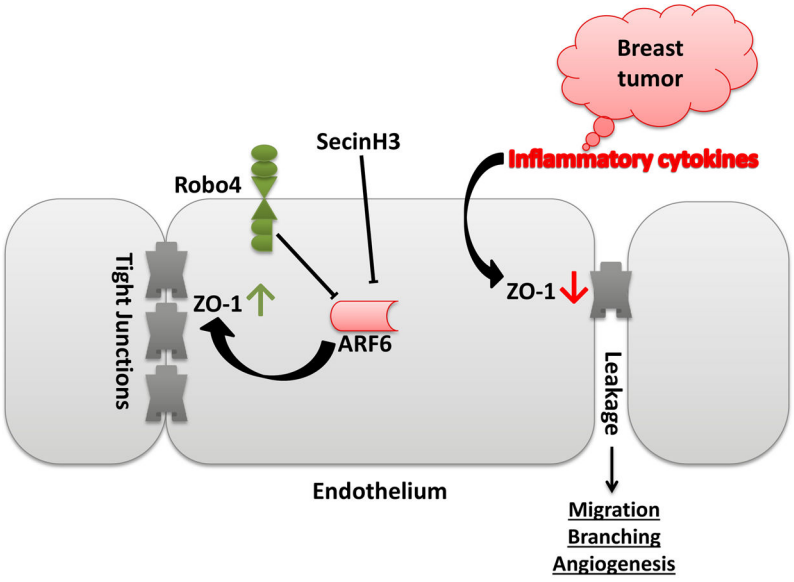

Figure 8.
Schematic illustration of the proposed mechanism.